

Laser Induced Shock Defects in Copper Aluminum Alloys: Stacking Fault Energy Effects on the Slip-Twinning Transition

M.S. Schneider^{1,a}, B.K. Kad¹, F. Gregori², D.H. Kalantar³
 B.A. Remington³ and M.A. Meyers^{1,b}

¹Department of Mechanical and Aerospace Engineering, University of California, San Diego,
 La Jolla, CA 92093-0411, USA

²Laboratory for Mechanical Properties and Thermodynamics of Materials, University of Paris 13,
 Villetaneuse, France

³Lawrence Livermore National Laboratory, Livermore, CA 94550, USA

^am1schneider@ucsd.edu, ^bmameyers@ucsd.edu

Keywords: Copper Aluminum, Laser-Shock, Shock-Induced Defects, Stacking Fault Energy

Abstract. Copper and copper aluminum (2 and 6 wt% aluminum) with two orientations, [001] and $\bar{1}134$, were subjected to high intensity laser shocks (energy levels of 40-300 J; energy densities of 15-70 MJ/m² and durations of 2.5 ns). The defects created were characterized by transmission electron microscopy. The slip-twinning transition was determined quantitatively in terms of both orientation and stacking fault energy. The threshold twinning pressure for copper oriented to [001] decreases with decreasing stacking fault energy from 40 GPa for pure copper to less than 20 GPa for copper-2 wt% aluminum. For the $\bar{1}134$ orientation, pure copper twinned at pressures on the order of 60 GPa, and whereas the copper-2 wt% aluminum alloy readily twinned at pressures less than 40 GPa. The results are rationalized in terms of a criterion in which slip and twinning are considered as competing mechanisms. A constitutive description using a modified MTS (mechanical threshold stress) constitutive equation applied incorporating slip and twinning in terms of orientation, stacking fault energy, temperature rise due to shock heating, and strain rate. The predictions are in agreement with experiments. The constitutive description provides a rationale for the experimental results; the calculated thresholds for [001] and $\bar{1}134$ are, respectively: 17 GPa and 25 GPa for pure copper, 9 GPa and 13 GPa, for Cu-2wt % Al and 1 GPa and 2 GPa for Cu-6wt% Al.

Introduction

The use of lasers to create shockwaves in metals was first demonstrated in 1963 by Askaryon and Morez [1] and further developed by Anderholm [2] through the use of a transparent overlay which confined the plasma formed at the surface from the laser-material interaction increasing the maximum achievable pressure. Since these early experiments, much work has been done to examine the effects of laser induced shocks on materials. Simultaneous shock compression and X-ray diffraction experiments were introduced by Johnson et al. [3] and continued by Zaretsky et al. [4]. Wark et al. [5] used laser-generated X-rays to produce shock compression at the NOVA

facility (LLNL). These shock compression experiments on silicon monocrystals were coupled with X-ray diffraction that successfully measured the compression both perpendicular (Laue) and parallel (Bragg) to the shock propagation direction. Fairand et al. [6] and Clauer et al. [7] used laser-induced shock pulses to modify the microstructure of engineering alloys, increasing their strength and fatigue resistance. Recent work by Meyers, et al. [8], Schneider, et al. [9], and Lubarda, et al. [10] has examined laser-induced shock defects in monocrystalline (high purity) copper as a function of pressure and orientation, as well as the nucleation, growth and coalescence of voids. This paper reports the extension of these experiments to copper-2 and -6 wt% aluminum for the [001] and $[\bar{1}34]$ orientations, and the compositional effect due to changing stacking fault energy on the slip-twinning transition.

Experimental Techniques

High intensity, pulsed lasers are an excellent way to study shock compression effects in solids since pressures on the order of a 100 GPa and strain rates above 10^7s^{-1} are possible. Three distinct techniques were applied during these experiments to obtain an in-depth understanding of shock effects in a crystalline material: in-situ dynamic X-ray diffraction, VISAR wave profile measurements and recovery experiments for defect analysis. The results from the X-ray diffraction experiments and VISAR measurements are described elsewhere [11].

For the recovery experiments, copper (99.999% pure) and copper-2 and -6 wt% aluminum single crystals with orientations [001] and $[\bar{1}34]$ were selected. The [001] orientation is highly symmetric whereas $[\bar{1}34]$ is asymmetric. The crystals were obtained from Goodfellow, Inc. in the form of 30 mm long rods with a 3 mm diameter. Samples were then cut by EDM (electro-discharge machining) into smaller rods with a 2.5 mm length. The surfaces were polished and the samples were mounted by press fitting into foam-filled recovery tubes.

The shock experiments were primarily carried out at the OMEGA Laser Facility at University of Rochester's Laboratory for Laser Energetics (LLE). The input laser energies used in the experiments were 70 J, 200 J, and 300 J for each orientation and composition. However, only the 200 J condition will be described herein. The laser spot size was on the order of 3 mm with a pulse duration of 2.5 ns. The energies can be translated into pressures using Lindl's equation [12]:

$$P = 4 \times 10^3 \left(\frac{I_{15}}{\lambda} \right)^{2/3} \quad (1)$$

where P is pressure (GPa), I_{15} is laser intensity (in 10^{15} W/cm^2), and λ is wavelength in micrometers. For example, for a laser pulse of 50 J with a pulse duration of 3 ns, a spot size of 0.001 m (1 mm), and the wavelength of the laser equal to 532 nm, one obtains an initial pressure of 100 GPa. For the experiments described herein, a laser energy of 200 J was used which is equivalent to 40 GPa. It is important to note that the pressure decays rapidly due to the short pulse duration as shown in Figure 1, which is a hydrocode calculation calibrated with VISAR profile measurements.

Post-mortem samples were recovered and systematically cut using EDM every 0.5 mm from the impact surface. The samples were mechanically ground to a thickness of 100 μm . The thin foils were prepared for TEM examination by an electro-polishing. TEM observation was conducted in a Philips CM-30 microscope operating at 300 kV or a JEOL 200CX operating at 200 kV.

The results of six shock recovery conditions are reported herein: two orientations and three compositions. The results obtained from pure copper in [001] and $[\bar{1}14]$ have been extensively discussed in Meyers et al. [8] and Schneider, et al. [9]. These will only be described briefly in order to compare the results of the differing orientations and compositions.

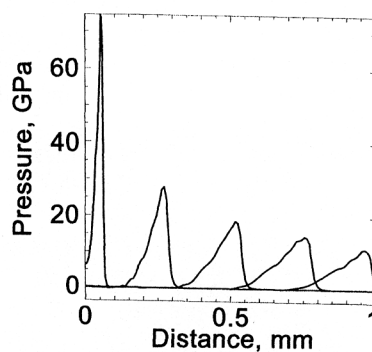


Figure 1 Simulated pressure profile in the sample at a laser shock energy 200 J.

Experimental Results

Copper has been the object of numerous shock recovery experiments and its response is fairly well understood at strain rates below 10^6 s^{-1} . It has a relatively high stacking-fault energy of $75 \pm 8 \text{ mJ/m}^2$, which is similar to nickel, but only 2/3 of aluminum. Because of the high stacking fault energy, twinning is inherently difficult to obtain in pure copper, requiring either low temperatures or high strain rates. Typically, in shock-compressed copper, the defect substructure consists of dislocation cells, e.g. see Murr [13], Grace [14] and Schneider, et al. [9]. When higher pressures are obtained, twinning becomes not only possible, but the dominant deformation mechanism. For single crystalline pure copper, De Angelis and Cohen [15] found that the crystal twinning pressure was 14 GPa for a shock wave propagating along [100] whereas it was 16 GPa for [111]. This is consistent with the findings by Nolder and Thomas [16, 17] for nickel.

By adding small amounts of aluminum ($< 7 \text{ wt\%}$) to the copper, it is possible to alter the stacking fault energy (SFE) and thereby characterize the effect of stacking fault energy on the threshold pressure for twinning. These systematic differences are observed in the deformation substructures for the two crystal orientations and different compositions: pure copper, copper-2 wt% aluminum and copper-6 wt% aluminum.

The unshocked copper crystal shows only a limited number of dislocations without preferred alignments or arrangements. The dislocation density is typically that of an un-deformed crystal (on the order of 10^8 m^{-2}).

Pure Copper. Impacting pure copper oriented to [001] with 205 J of energy created dense dislocation tangles, stacking faults and micro-twins. There are no readily discernible dislocation cells. The tangles were made of primarily $1/2\langle 110 \rangle$ dislocations. These traces (Figure 2(a)) were characteristic of stacking-fault bundles and twins which are analogous to previous observations by Murr [13], especially, Figs. 20, 21, and 23 of [6]. Furthermore, the observed deformation substructure appeared uniform around the thin foil perforation. These features were significantly different than the deformation substructure observed at the lower laser impact energies [8]. Perpendicular traces of planar features were seen when the beam direction is $\langle 001 \rangle$. These

correspond to traces of $\{111\}$ on (001) . All four stacking fault variants *viz* the partial dislocations $(11\bar{1})1/6[112]$, $(111)1/6[\bar{1}\bar{1}2]$, $(\bar{1}\bar{1}1)1/6[1\bar{1}2]$, and $(\bar{1}\bar{1}1)1/6[\bar{1}12]$ were observed. Given the incident energy input as parallel to $[001]$, it is not surprising that all four stacking fault variants were activated, Figure 7(a), as they all have the same Schmid factor, 0.4082. Figure 7(a) shows stacking faults and dislocation tangles marked as DT and SF.

For the $[\bar{1}34]$ orientation shocked at 40 GPa, the deformation substructure was cellular, with an average cell size of $0.15 \pm 0.05 \mu\text{m}$ and a dislocation density on the order of 10^{14} m^{-2} , Figure 2(b). This is in direct contrast to the high density of stacking faults observed in $[001]$. The cells were comprised predominantly by three dislocation systems: one primary system, $(111)[\bar{1}01]$, with a Schmid factor of 0.4711, and two secondary systems $(111)[\bar{1}\bar{1}0]$ and $(\bar{1}\bar{1}1)[101]$ with a Schmid factor of 0.3768. Additional slip systems were activated since the resolved shear stress due to the pressure wave exceeds the dynamic yield strength for these dislocation systems. However, it was observed that the contribution to the dislocation density from these other slip systems is relatively small compared to the dislocations associated with the primary and secondary slip systems with much higher Schmid factors. A large number of loops were also visible are found to contribute to the cell walls and were commonly observed within the cells in a very low concentration.

Copper-2 wt% Aluminum. As expected, in the Cu-2wt% Al $[001]$ copper shocked at 200 J, twinning readily occurred as shown in Figure 3(a). Because of the 2wt% addition of aluminum, the stacking fault energy is less than $\frac{1}{2}$ of pure copper. At least two variants (and possibly four) were observed. They were both well defined and appear to have a regular spacing of 250 nm. When imaged at $B = [001]$, they appeared at exactly 90° to each other aligned along $[220]$ and $[\bar{2}20]$ directions. They were present in roughly the same proportion. The overall density of twins was high as shown in the micrograph. The twins varied in size and length with an average width of 50-100 nm and length on the order $1 \mu\text{m}$. A large number of dislocations were also observed between the twins, which are not common in pure copper when shocked at pressures above the twinning threshold. It was difficult to determine a dislocation density with the high twinning density, but a density on the order of 10^{12} m^{-2} could be approximated by comparing several samples.

The results obtained for Cu-2wt Al oriented to $[\bar{1}34]$ showed two twinning variants activated where the domain of one twin may be the nucleation site for the secondary twinning system (Figure 3(b)). The twins were in lower proportions than expected. The twins varied in size

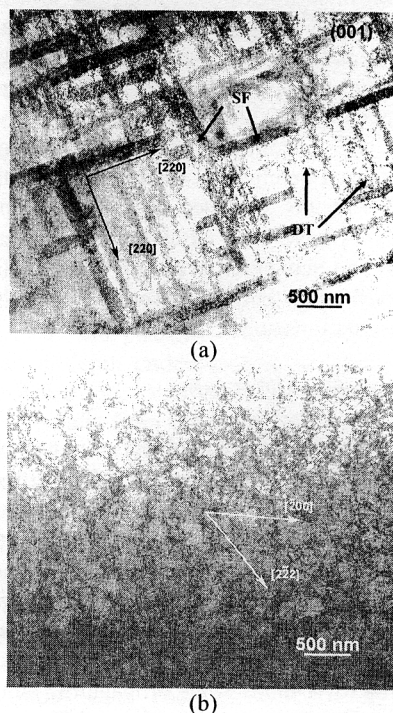


Figure 2 Pure Cu shocked with laser energy of 200 J; (a) $[001]$ orientation, $B = [001]$; (b) $[\bar{1}34]$, $B = [011]$.

and proportion with the primary variant, $(111)[\bar{2}11]$, having an average length of $4\ \mu\text{m}$ and a width of 20-30 nm. The secondary variant, $(1\bar{1}1)[\bar{1}\bar{1}\bar{2}]$, was greater in number, but shorter in length with an average of $2\ \mu\text{m}$. In this system, the primary twinning system has a Schmid factor of 0.4895

and the secondary system, 0.3857. It was expected that a co-secondary twinning variant would also be found, $(1\bar{1}1)[1\bar{1}\bar{2}]$, but the occurrence of this system was relatively rare. This suggests that the sample may have been slightly misaligned from the $[\bar{1}34]$ loading axis, and thereby preferred the observed twinning systems. A high density of dislocations was also observed in the samples (not visible here). These were found as tangles, loops, and a transitional structure between planar arrays and cells. The dislocation density was lower than in pure copper likely as a result of twinning.

Copper-6 wt% Aluminum. Dislocations, stacking faults, and twins were all observed in the Cu-6 wt% Al oriented to $[001]$. For this system, the stacking fault energy is nearly zero. The dislocation structure consisted of large planar arrays and regions of dislocation pileup since the low stacking fault energy inhibits cross-slip. The dislocations were primarily partials of the type $\{111\}1/6\langle 112\rangle$ or what are commonly known as Shockley partials. They are glissile on $\{111\}$ planes. These dislocations form when $1/2\langle 110\rangle$ dislocations dissociate into $1/6\langle 112\rangle$ forming the boundaries of the stacking faults as observed in Figure 4(a). It is expected that these faults are intrinsic faults of low energy configuration due to shear forces on the close packed $\{111\}$ planes. The faults are separated by an average distance of 500 nm and vary greatly in length from 500 nm to several microns. The fault width varies from 20 nm to 200 nm. Twinning was observed at lower proportions than expected, being spaced sporadically in the specimen (not shown). Each of the four variants of twinning as calculated by Schmid factors was observed.

For the $[\bar{1}34]$ orientation of the Cu-6 wt% Al, three variants of stacking faults were observed as imaged in Figure 4(b). Often it was found that the close intersection of these faults formed stacking fault tetrahedral. An in-depth analysis of the formation of the stacking fault tetrahedra is ongoing, but it is likely that they are the result of gliding screw dislocations. There was one primary stacking fault orientation observed which has the greatest width, $\sim 250\ \text{nm}$, and an average length of $5\ \mu\text{m}$. Two secondary systems as suggested by Schmid factors also are observed in equivalent amounts. They have widths on the order of 50 nm and lengths of an average $2\ \mu\text{m}$. Twinning also was observed, though only in the primary system, $(111)[\bar{2}11]$.

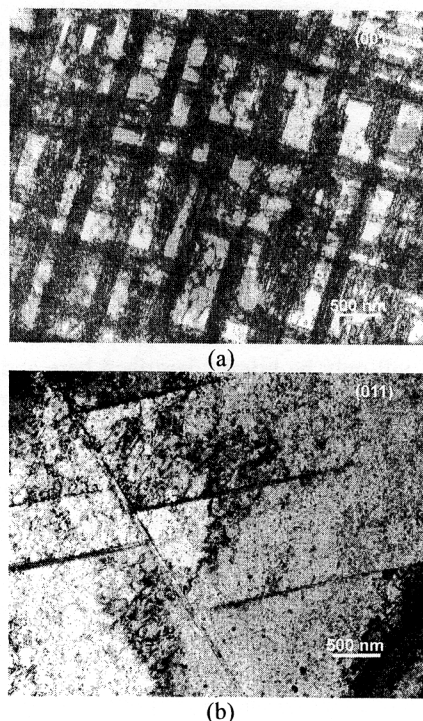


Figure 3 Cu-2 wt% Al shocked with laser energy of 200 J; (a) $[001]$, $B = [001]$; (b) $[\bar{1}34]$, $B = [011]$.

Analysis of the Slip-Twinning Transition in High Strain Rate Deformation

The existence of a twinning threshold at high pressures and high strain rates in FCC metals is well documented, but limited work has been done to quantify this behavior in terms of orientation and SFE. Part of the difficulty is the less than adequate theoretical understanding which exists to explain the deformation mechanism transition. One of the major goals of the current research is to develop a better constitutive description of the monocrystals and to correlate the experimentally obtained twinning threshold stress with theoretical predictions. The methodology to be used in the prediction of the threshold shock amplitude was delineated by Murr et al. [18] and Meyers et al. [19] and will only be briefly described here and then applied to the different conditions previously described.

Stacking Fault Energy Suzuki and Barrett [20] and Venables [21, 22] proposed relationships between the SFE (γ_{SF}) and the twinning stress, τ_T . It is well known that the twinning stress increases with increasing SFE. This is true mostly for FCC metals as shown by Narita, et al. [23], and the classic plot by Venables [21, 22] shows this effect very clearly. Based on the analysis of a number of FCC materials, Narita and Takamura [24]

found that γ_{SF} and τ_T are proportional, and proposed that $\gamma_{SF} = 2b_s \tau_T$, where b_s is the Burgers vector for a Shockley partial. Gallagher [25] and Vöhringer [26] correlated the SFE to the electron/atom (e/a) ratio in copper alloys and arrived at the following expression

$$\ln\left(\frac{\gamma_{SF}}{\gamma_{Cu}}\right) = K_1 \left(\frac{C}{C + C_{max}}\right)^2 \quad (2)$$

where γ_{Cu} is the stacking fault energy for copper, and C is the concentration of solute atoms. The maximum concentration of the solute is denoted by C_{max} . The best fit was obtained with $K_1 = 12.5$ and $\gamma_{Cu} = 78 \pm 8$ mJ/m². Equation (18) can be combined with the mathematical representation of data as shown in Figure 5, which is a compilation of results by Venables [21] and Vöhringer [27]. The twinning stress for a number of copper alloys is shown to vary with the square root of the SFE:

$$\sigma_T = K_2 \left(\frac{\gamma_{SF}}{Gb}\right)^{1/2} \quad (3)$$

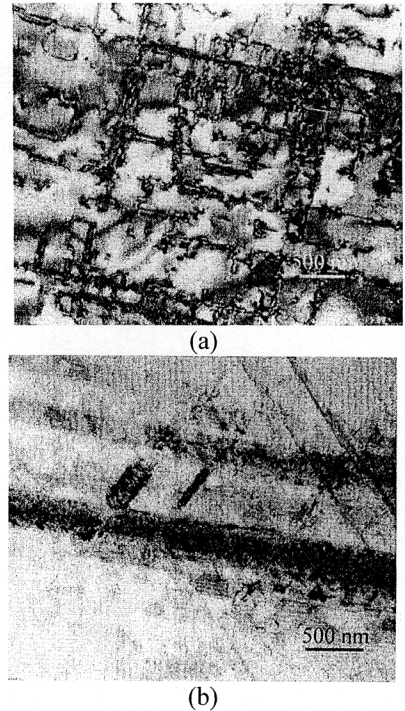


Figure 4 Cu-6 wt% Al shocked with laser energy of 200 J; (a) [001], B = [001]; (b) [134], B = [011].

A good fit is obtained with $K_2 = 6$ GPa. The same fit was satisfactorily obtained by Narita and Takamura [11] for Ni-Ge alloys. Substitution of equation (18) into equation (19) yields

$$\sigma_T = \frac{K_2}{Gb^{1/2}} \exp \left[\ln \gamma_{Cu} + K_1 \left(\frac{C}{C + C_{max}} \right)^2 \right]^{1/2} \quad (4)$$

Slip-Twinning Threshold. One can obtain the critical stress for the slip-twinning transition as a function of SFE, ϵ , $\dot{\epsilon}$, and T . The application of this criterion to the shock front necessitates the knowledge of the strain rate. The strain rate at the shock front has been established by Swegle and Grady [28] to be, as a function of pressure, P :

$$P = k_{SG} \dot{\epsilon}^{1/4} \quad (5)$$

where k_{SG} is an empirical parameter.

Two separate aspects have to be considered in the analysis: (a) shock heating and (b) plastic strain at the shock front. Both shock heating and plastic strain by slip (and the associated work hardening) alter the flow stress of material by slip processes and need to be incorporated into the computation. For a thorough treatise on this, see Meyers, et al. [8] Inserting Eqn. 5 into the P-V Hugoniot relationship, one obtains:

$$P = \frac{C_0^2 (1 - e^\epsilon)}{V_0 [1 - S(1 - e^\epsilon)]^2} \quad (6)$$

The constitutive response of the material is represented by the modified MTS expression below:

$$\sigma_s = \sigma_0 f(\epsilon) \left[1 - \left(\frac{kT}{Gb^3 g_0} \ln \left(\frac{\dot{\epsilon}_0}{\dot{\epsilon}} \right) \right)^{2/3} \right]^2 \quad (7)$$

where $f(\epsilon)$ is an experimentally determined work hardening term fitted with a high-order polynomial. By applying Eqn. 7, in conjunction with Eqns. 4-6, one obtains the threshold twinning pressure. At ambient temperature, the threshold twinning pressures for the $[1\bar{1}34]$ orientation are 25 GPa for pure copper, 12.5 GPa for Cu-2 wt% Al, and <2 GPa for Cu-6 wt% Al; whereas the threshold pressures for $[001]$ are 17 GPa for pure copper, 8.5 GPa for Cu-2 wt% Al, and 1 GPa for Cu-6 wt% Al as shown in Figure 6. This is the first quantitative prediction analysis for the

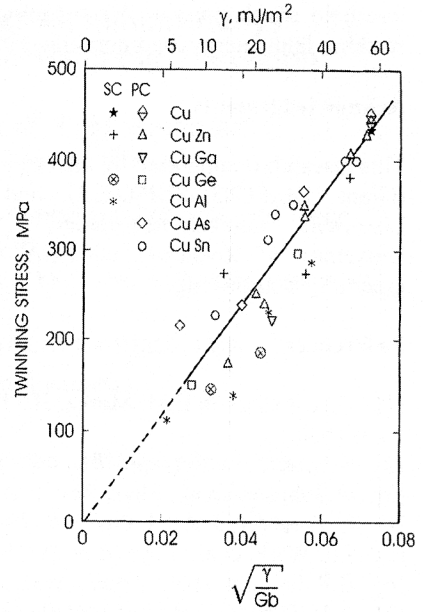


Figure 5 Twinning stress as a function of SFE for copper and copper solid solutions.

threshold shock pressure for twinning dependence on stacking fault energy incorporating orientation effects.

Acknowledgements

This research is supported by the Department of Energy (Grant DE-FG03-98DP00212) and by Lawrence Livermore National Laboratory. The use of the University of Rochester OMEGA Laser facility is gratefully acknowledged.

References

- [1] G.A. Askaryon E.M. Morez: JETP Lett. 16 (1963), p.1638.
- [2] N.C. Anderholm: Appl. Phys. Lett. 12 (1970), p.113.
- [3] Q. Johnson, et al.: Phys. Rev. Lett. 25 (1970), p.109.
- [4] E. Zaretsky: J. Appl. Phys. 78 (1995), p.1.
- [5] J.S. Wark, et al.: Phys. Rev. B 40 (1989), p. 5705.
- [6] B.P. Fairand, et al.: Appl. Phys. Lett. 25 (1974), p.431.
- [7] A.H. Clauer, et al.: in *Shock Waves and High-Strain-Rate Phenomena in Metals*, (eds. M.A. Meyers and L.E. Murr, Plenum, NY 1981, p.675.)
- [8] M.A. Meyers, et al.: Acta Mat. 51 (2003) p.1211.
- [9] M.S. Schneider, et al.: Met Trans A, Accepted for publication 2003.
- [10] V.A. Lubarda, et al.: Acta Mat., Accepted for publication 2003
- [11] Kalantar, D.H., et al. Phys. Plas., 10 (2003), p. 1569.
- [12] J. Lindl: Phys. Plasmas 2 (1995), p. 3933.
- [13] L.E. Murr: *Shock Waves and High-Strain-Rate Phenomena in Metals* (eds. M.A. Meyers and L.E. Murr, Plenum, NY, 1981, p.607.)
- [14] F.I. Grace: J. Appl. Phys. 40 (1969), p.2649.
- [15] R.J. De Angelis and J.B. Cohen: J. of Metals 15 (1963), p.681.
- [16] R.L. Nolder and G. Thomas: Acta Met. 11 (1963), p.994.
- [17] R.L. Nolder and G. Thomas: Acta Met. 12 (1964), p.227.
- [18] L.E. Murr, et al.: Acta Mater. 45 (1997), p.157.
- [19] M.A. Meyers, et al.: Acta Mat 49 (2001) p.4025.
- [20] H. Suzuki and C. S. Barrett: Acta metall. 6 (1958), p.156.
- [21] J. A. Venables: Phil. Mag. 6 (1961), p.379.
- [22] J. A. Venables: in *Deformation Twinning* (Gordon & Breach, New York, 1964, p.77.)
- [23] N. Narita, et al.: J. Japan Inst. Met. 42 (1978), 533.
- [24] N. Narita and J. -I. Takamura: in *Dislocations in Solids* Vol. 9 (Elsevier, Amsterdam, 1992)
- [25] P. C. Gallagher: J., *Metall. Trans.* 1 (1970), p.2429.
- [26] O. Vöhringer: *Metall.* 11 (1972), p.1119.
- [27] O. Vöhringer: *Z. Metallk.* 65 (1974), p.352.
- [28] J.W. Sweigle and D.E. Grady: J. Appl. Phys. 58 (1985), p.692.

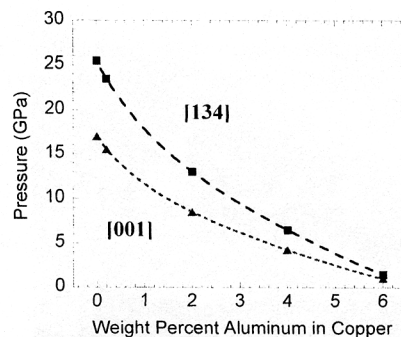


Figure 6 Calculated shock pressures required to produce twinning in the Cu-Al system for the [001] and [134] orientations